

# Description of PVT Behavior of an Industrial Polypropylene–EPR Copolymer in Process Conditions

R. PANTANI, G. TITOMANLIO

Department of Chemical and Food Engineering, University of Salerno, Via Ponte don Melillo, 84084 Fisciano SA, Italy

Received 8 March 2000; accepted 29 May 2000

**ABSTRACT:** An experimental procedure is presented to describe the PVT behavior of multiphase polymeric materials in a wide range of cooling rates. In particular, the procedure is applied to a typical multiphase industrial polymer, that is, an industrial polypropylene–ethylene-propylene rubber (iPP–EPR) copolymer with a small percentage of talc. The volume evolution is described combining specific volumes of different phases present in the material. All phases are described simply by thermal expansion and compressibility coefficients drawn either from the literature or from low and high temperature (i.e., below and above the iPP crystallization range) standard PVT data. Crystallization evolution of iPP is described by the Nakamura nonisothermal formulation of the Avrami–Evans crystallization kinetic model. Model parameters are identified by comparison with both standard calorimetric results and final densities of thin samples solidified during quenches conducted with cooling rates of several hundreds of K/s. It is also shown that identification of crystallization kinetic parameters by means of calorimetric data only leads to misleading results for cooling rates larger than those adopted in the calorimetric tests. © 2001 John Wiley & Sons, Inc. *J Appl Polym Sci* 81: 267–278, 2001

**Key words:** iPP–EPR copolymer; PVT; crystallization kinetics

## INTRODUCTION

A good description of polymer volume is one of the basic challenges for the polymer processing industry, to predict important features of an injection-molding cycle (such as, for instance, pressure curves) and final product characteristics in terms of dimensional accuracy and postprocessing volume relaxation.<sup>1</sup>

Polymer density is strongly influenced by cooling conditions such as cooling rate and pressure history, and this is particularly true for semicrys-

talline polymers. In fact, during cooling from the molten state, this class of materials undergoes a transition from a completely amorphous to a partially crystalline status, which results in a major change of all material characteristics, including volumetric parameters.

Polymeric materials are often quite complex because they include several phases, each of them being optimized to improve either processing performance or final product properties. Standard tests to describe polymer volume during cooling are confined to unreasonably low cooling rates and/or pressure, if compared with those experienced by the material during processing. In this work a procedure is presented to describe the pressure–volume–temperature (PVT) behavior of multiphase polymeric materials over a wide range of cooling rates. This procedure is based on

Correspondence to: R. Pantani (pantani@dica.unisa.it)

Contract grant sponsor: CNR (Progetto Finalizzato su Materiali Speciali per Tecnologie Avanzate).

*Journal of Applied Polymer Science*, Vol. 81, 267–278 (2001)  
© 2001 John Wiley & Sons, Inc.

**Table I** Values of Parameters Appearing in Eq. (1), as Taken From the C-Mold 99.1 Database, Describing the Equilibrium PVT Behavior of Montell BA 238 G3

Parameter	$B1_m$ (m <sup>3</sup> /kg)	$B2_m$ (m <sup>3</sup> /kg K)	$B3_m$ (Pa)	$B1_s$ (m <sup>3</sup> /kg)	$B2_s$ (m <sup>3</sup> /kg K)	$B3_s$ (Pa)	
Value	$1.275 \times 10^{-3}$	$10^{-6}$	$8.66 \times 10^7$	$1.184 \times 10^{-3}$	$6 \times 10^{-7}$	$1.47 \times 10^8$	
Parameter	$B4_m$ (1/K)	$B4_s$ (1/K)	$B5$ (K)	$B6$ (K/Pa)	$B7$ (m <sup>3</sup> /kg)	$B8$ (1/K)	$B9$ (1/Pa)
Value	$5.181 \times 10^{-3}$	$4.589 \times 10^{-3}$	428.15	$7.18 \times 10^{-8}$	$9.07 \times 10^{-5}$	0.12564	$1.21 \times 10^{-8}$

the analysis of crystallization kinetic behavior at cooling rates as high as several hundreds of degrees per second, as described in Brucato et al.<sup>2</sup>

Knowing crystallization kinetics, it will be possible to obtain not only specific volume evolution from cooling history during processing, but also the evolution of macroscopic crystallinity degree, which influences all properties of the final object and other features of interest to polymer processing such as distribution of melt–solid transition temperature.

The procedure in this work is applied, rather than to a simple pure model material, to a typical industrial material, that is, an industrial polypropylene–ethylene-propylene rubber (iPP–EPR) copolymer with a small percentage of talc. The purpose of such a choice is that of facing, and pointing out during the investigation, all the problems related to a complex material formulation.

## EXPERIMENTAL

### Material

A semicrystalline polymer (HIFAX BA 238 G3, kindly supplied by Montell, Ferrara, Italy) was selected as the testing material. It is a heterophasic polypropylene with an excellent stiffness/impact strength balance. Impact strength is improved by an ethylene-propylene rubber phase (EPR, copolymer C<sub>2</sub>–C<sub>3</sub> at about 50% of each component) dispersed in the polypropylene matrix; rubber weight percentage is about 26%<sup>3</sup>; a small percentage of talc (about 1.5%) is also present in the resin.

### Equilibrium PVT Behavior

Material PVT behavior in equilibrium conditions was taken from the C-Mold 99.1 of the AC Technology database. The C-Mold database<sup>4</sup> refers to a characterization procedure based on isothermal compression volume change measurements,

starting at each temperature from room pressure. The PVT behavior explored as specified above was described by AC Technology by means of the following modified form of the Tait equation<sup>4</sup>:

$$v(T, P) = v_0(T) \left[ 1 - C \ln \left( 1 + \frac{P}{B(T)} \right) \right] + v_r(T, P) \quad (1)$$

with  $C = 0.0894$  and

	If $T > T_r(P)$	If $T < T_r(P)$
$v_0(T) =$	$B1_m + B2_m T_c$	$B1_s + B2_s T_c$
$B(T) =$	$B3_m \exp(-B4_m T_c)$	$B3_s \exp(-B4_s T_c)$
$v_r(T, P) =$	0	$B7 \exp(B8T - B9P)$
$T_c = T - B5$		
$T_r(P) = B5 + B6P$		

The values of parameters to be used in eq. (1) for Montell BA 238 G3 are listed in Table I. In the following, the values of specific volume calculated by eq. (1) will be reconciled to experimental results obtained by AC Technology by the procedure described above.

### Calorimetry

Some samples of material were solidified in a DSC apparatus (Mettler, Griefensee, Switzerland), with liquid nitrogen as cooling fluid, under different cooling rates (in the range 1–80 K/min). All samples were kept at a temperature of 503 K for 30 min and then cooled down according to the test procedure. Calorimetric curves obtained under constant cooling rates are shown in Figure 1. By increasing the cooling rate, all curves shift toward lower temperatures and crystallization develops over a wider temperature range. The overall heat released during solidification does not change significantly by changing cooling rate (at least in the range used for these experiments) and has been found to scatter between 73 and 80 J/g.

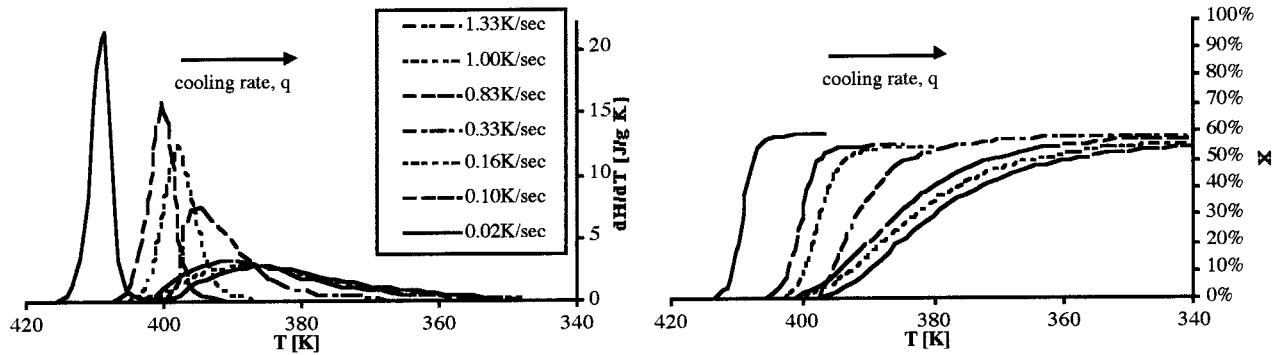


**Figure 1** Calorimetric curves measured during solidification of BA 238 G3 samples in a DSC apparatus at different cooling rates.

The final degree of crystallinity of the iPP phase (representing 72.5% of total samples mass) in the samples solidified with DSC ramps was found from calorimetric curves by using  $\lambda = 1.88 \times 10^5$  J/kg as the latent heat of crystallization.<sup>5</sup> In the range of the cooling rates investigated, the crystallinity degree was always found to be between 54 and 59%.

Four samples were analyzed in a DSC apparatus (Perkin–Elmer, Foster City, CA), using nitrogen as cooling gas under isothermal conditions. Also in this case the samples were kept for about 30 min at 503 K before lowering the temperature at a rate of 1 K/s to the test value. The material was tested at four temperatures: 410, 413, 416, and 418 K. At higher temperatures, testing times were very high and output signals too low, whereas lower temperatures could not be reached because of the limited apparatus cooling rate, which was not sufficient to prevent samples from crystallizing during cooling to set temperature. Calorimetric curves are shown in Figure 2. The overall energy released during each isothermal test was always found to be between 72 and 80

J/g, consistent with the above-noted results of calorimetric cooling ramps. Half-crystallization times (i.e., the times that crystallinity reaches one-half the equilibrium value) increase with the temperature of the isothermal test.

#### Quenching of Thin Samples

An experimental technique, which is an evolution of the one presented in Brucato et al.,<sup>2</sup> was adopted to carry out the characterized solidification quenches of thin molten polymer films. The thermal history experienced by the sample was measured during the quenches by means of a thin thermocouple connected to a fast data acquisition system. The scheme of experimental apparatus adopted for the cooling procedure is depicted in Figure 3; it is similar to the first one, developed at the University of Palermo, and consists of a sample holder made by two thin copper slabs linked to a rod that can slide vertically, bringing the sample from an oven, in the upper part of the apparatus, to the lower part, where a cooling fluid is sprayed against the copper slabs. The two copper

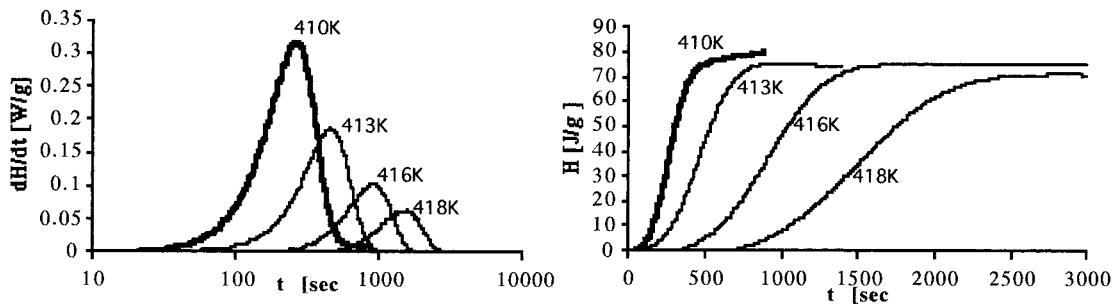


**Figure 2** Calorimetric curves obtained during isothermal analysis at different temperatures of samples of Montell BA 238 G3 in a DSC apparatus.

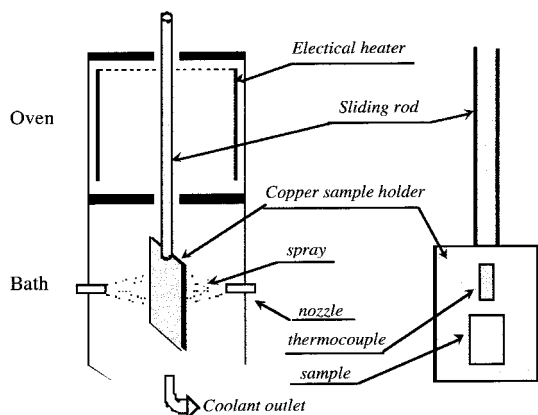


**Figure 3** Layout of the experimental apparatus used for controlled cooling histories.

slabs were 0.5 mm thick and the thickness of the polymer sample was always smaller than 0.1 mm; contact between copper walls and polymer was ensured by means of elastic pincers. Temperature evolution was monitored by the thin thermocouple located in the copper holders close to the sample. Values of the Biot number were estimated to be smaller than 0.1 (up to the highest cooling rate attained), with reference to both the polymer sample and the copper holder; thus, thermocouple readings could be considered representative of a homogeneous temperature inside the polymer.

Samples were kept at 503 K for 30 min and then cooled to room temperature. Typical thermal histories obtained with this procedure are reported in Figure 4, together with the corresponding cooling rates; cooling histories of DSC ramps are also added for comparison.

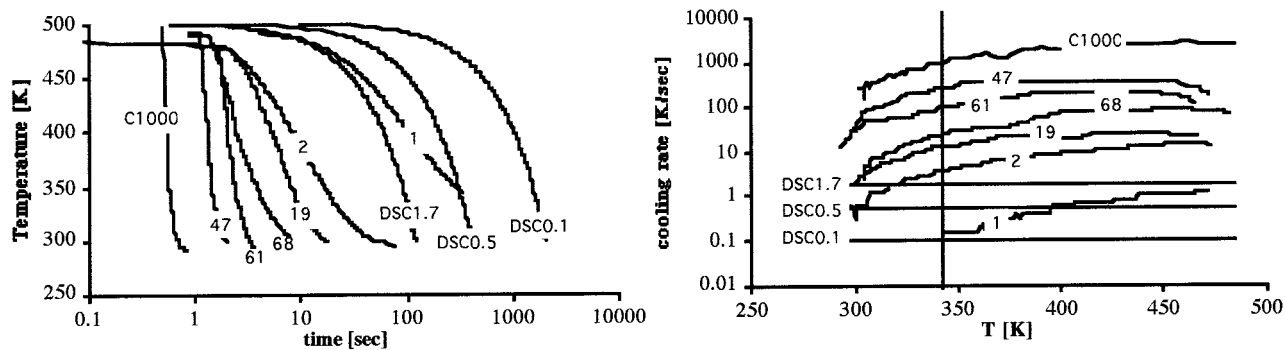


**Figure 4** Cooling histories of some of the samples listed in Table II. Samples indicated with "DSC" were solidified in a DSC apparatus. Sample indicated with "C" was solidified at University of Palermo. Line at 343 K is a reference for the characteristic temperature for iPP crystallization at high cooling rates, as specified in Piccarolo et al.<sup>6</sup>

### Density Measurements in Gradient Columns

Specific volumes of samples solidified in different conditions were measured in density-gradient columns prepared with solutions of ethyl alcohol and water. The density of the samples was measured at 298 K and, for a few of them, also at 318 and 278 K.

To shorten the measurement time after solidification, the sample specific volume about 10 min after quenching was evaluated by analyzing the falling velocity curve versus position inside the column.<sup>2</sup> Results of specific volume measurements are shown in Table II. Measurements taken when sample reached hydrodynamic equilibrium inside the column (i.e., after 1 h at 318 K, 3 h at 298 K, and 10 h at 278 K) are also reported in Table II.

Dependency of specific volume (measured at 298 K) on cooling rate is shown in Figure 5, which clearly shows that the volume starts to increase from a value of about  $1.120 \times 10^{-3} \text{ m}^3/\text{kg}$  only at rates higher than about 100 K/s.

To obtain dilatometric measurements at low temperatures, two samples were solidified at cooling rates of 0.02 and 10 K/s and were allowed to age at 318 K for about 200 h. Their specific volumes were then measured at 318, 298, and 278 K, by changing column coolant temperature. A second cycle of temperature changes was then performed to test reproducibility. The time needed to reach thermal equilibrium for the column at the new test temperature was about 1 h. The whole measurement time was about 10 h. Results, shown in Table III, confirming good reproducibility between the first and second temperature cy-

**Table II Overview of Specific Volume Measurements Performed**

Sample <sup>a</sup>	<i>T</i> Column (K)	<i>q</i> at 343 K (K/s)	Aging Time <sup>b</sup> (s)	Specific Volume (m <sup>3</sup> /kg)	<i>x</i> (%) (iPP Phase) <sup>c</sup>	Aging Time <sup>b</sup> (s)	Specific Volume (m <sup>3</sup> /kg)	<i>x</i> (%) (iPP Phase) <sup>c</sup>
DSC0.1	298	0.1	600	1.118 × 10 <sup>-3</sup>	61	10,800	1.115 × 10 <sup>-3</sup>	64
1	298	0.1	600	1.124 × 10 <sup>-3</sup>	55	10,800	1.124 × 10 <sup>-3</sup>	55
75	298	0.2	600	1.123 × 10 <sup>-3</sup>	55	10,800	1.122 × 10 <sup>-3</sup>	57
43	298	0.2	600	1.124 × 10 <sup>-3</sup>	54	10,800	1.122 × 10 <sup>-3</sup>	56
DSC0.5	298	0.5	600	1.120 × 10 <sup>-3</sup>	58	10,800	1.119 × 10 <sup>-3</sup>	60
DSC1.7	298	1.7	600	1.118 × 10 <sup>-3</sup>	61	10,800	1.118 × 10 <sup>-3</sup>	60
19	298	13	600	1.124 × 10 <sup>-3</sup>	54	10,800	1.121 × 10 <sup>-3</sup>	57
2	298	3.6	600	1.123 × 10 <sup>-3</sup>	55	10,800	1.120 × 10 <sup>-3</sup>	59
40	298	15	600	1.121 × 10 <sup>-3</sup>	57	10,800	1.120 × 10 <sup>-3</sup>	59
30	298	60	600	1.123 × 10 <sup>-3</sup>	55	10,800	1.121 × 10 <sup>-3</sup>	57
39	298	100	600	1.128 × 10 <sup>-3</sup>	50	10,800	1.126 × 10 <sup>-3</sup>	53
41	298	110	600	1.129 × 10 <sup>-3</sup>	49	10,800	1.127 × 10 <sup>-3</sup>	51
36	298	121	600	1.125 × 10 <sup>-3</sup>	53	10,800	1.123 × 10 <sup>-3</sup>	55
38	298	161	600	1.130 × 10 <sup>-3</sup>	48	10,800	1.129 × 10 <sup>-3</sup>	49
37	298	273	600	1.129 × 10 <sup>-3</sup>	49	10,800	1.128 × 10 <sup>-3</sup>	50
47	298	294	600	1.133 × 10 <sup>-3</sup>	44	10,800	1.131 × 10 <sup>-3</sup>	47
C400	298	434	600	1.133 × 10 <sup>-3</sup>	45	10,800	1.132 × 10 <sup>-3</sup>	45
C600	298	600	600	1.134 × 10 <sup>-3</sup>	44	10,800	1.133 × 10 <sup>-3</sup>	44
C850	298	877	600	1.135 × 10 <sup>-3</sup>	42	10,800	1.135 × 10 <sup>-3</sup>	42
C900	298	950	600	1.131 × 10 <sup>-3</sup>	46	10,800	1.131 × 10 <sup>-3</sup>	47
C1000	298	1130	600	1.135 × 10 <sup>-3</sup>	43	10,800	1.134 × 10 <sup>-3</sup>	43
DSC0.02	318	0.02	600	1.135 × 10 <sup>-3</sup>	55	3600	1.133 × 10 <sup>-3</sup>	57
DSC0.1	318	0.1	600	1.135 × 10 <sup>-3</sup>	55	3600	1.133 × 10 <sup>-3</sup>	57
75	318	0.2	600	1.134 × 10 <sup>-3</sup>	55	3600	1.132 × 10 <sup>-3</sup>	57
DSC0.5	318	0.5	600	1.129 × 10 <sup>-3</sup>	61	3600	1.126 × 10 <sup>-3</sup>	64
DSC1.7	318	1.7	600	1.135 × 10 <sup>-3</sup>	55	3600	1.133 × 10 <sup>-3</sup>	57
68	318	23	600	1.129 × 10 <sup>-3</sup>	60	3600	1.126 × 10 <sup>-3</sup>	63
77	318	78	600	1.138 × 10 <sup>-3</sup>	51	3600	1.134 × 10 <sup>-3</sup>	56
76	318	149	600	1.136 × 10 <sup>-3</sup>	54	3600	1.129 × 10 <sup>-3</sup>	60
74	318	216	600	1.146 × 10 <sup>-3</sup>	44	3600	1.143 × 10 <sup>-3</sup>	47
73	318	326	600	1.144 × 10 <sup>-3</sup>	45	3600	1.142 × 10 <sup>-3</sup>	48
DSC1.7	278	1.7	600	1.101 × 10 <sup>-3</sup>	57	36,000	1.1091 × 10 <sup>-3</sup>	58
51	278	17	600	1.115 × 10 <sup>-3</sup>	52	36,000	1.112 × 10 <sup>-3</sup>	55
61	278	95	600	1.117 × 10 <sup>-3</sup>	49	36,000	1.115 × 10 <sup>-3</sup>	51
48	278	279	600	1.120 × 10 <sup>-3</sup>	46	36,000	1.119 × 10 <sup>-3</sup>	47
47	278	294	600	1.123 × 10 <sup>-3</sup>	42	36,000	1.121 × 10 <sup>-3</sup>	44
64	278	383	600	1.124 × 10 <sup>-3</sup>	40	36,000	1.120 × 10 <sup>-3</sup>	45

<sup>a</sup> Samples whose names start with “DSC” were solidified at constant cooling rates in a DSC apparatus. Samples whose names start with “C” were solidified at University of Palermo.

<sup>b</sup> Aging time refers to time elapsed inside the columns after solidification.

<sup>c</sup> Crystallinity degree was calculated by eqs. (2) and (4).

cles, exclude relevant changes during the measurement and can be used to obtain the thermal expansion coefficient, which was evaluated to be about  $4 \times 10^{-4} \text{ K}^{-1}$ .

### Optical Microscopy

Samples solidified under different cooling rates were analyzed by polarized light optical micros-

copy. A micrograph of the sample solidified at 0.1 K/s is shown in Figure 6(a): a spherulitic structure is evident and, within it, the rubber forms a dispersed phase with domains of an average dimension smaller than  $50 \mu$ . Only isolated birefringent spots in a noncrystalline matrix were observed in the samples solidified under high cooling rates; a micrograph of the sample solidi-



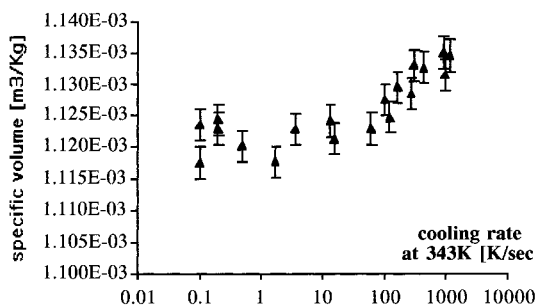


**Figure 5** Dependency of the specific volume on cooling rates (measured at 343 K). Measurements were taken at 298 K, 10 min after solidification.

fied at 294 K/s is shown in Figure 6(b): the birefringent spots can be related either to talc or to crystallinity seeds.

## RESULTS AND DISCUSSION

Material PVT behavior, as characterized by standard procedures, and also by the one used by AC Technology, does not account for time effects. Indeed, the Tait equation adopted for the description of AC Technology data, as pointed out in Pantani and Titomanlio<sup>7</sup> does not even account for cooling rate. On the other hand, it is well known that density of all polymeric materials is determined by the complete thermomechanical history, starting from the melt. The effect on specific volume of thermal history, experienced during solidification from the melt, is particularly relevant for semicrystalline polymers because

this class of materials undergoes partial crystallization during solidification and crystals have larger densities than that of those during the amorphous phase. Depending on crystallization kinetics, crystallinity evolution with temperature depends on the whole history experienced by the polymer during cooling from the melt. This effect parallels the effect of thermomechanical history on density contribution of the amorphous phase, which, however, has less relevance.

As shown, for instance in Figure 1, the temperature range in which crystallization takes place (i.e., the transition zone) changes, depending on the cooling rate; however, except for very high cooling rates and very long aging times, for iPP it takes place within the temperature range 330–430 K. Outside this range, on a first-approximation basis, crystallinity can be considered constant and the analysis of PVT behavior simplifies; obviously, crystallization kinetics determine the main features of density evolution inside the crystallization temperature range.

Consequently, the present analysis is split into three parts:

1. Combination of specific volume of each phase into the specific volume of the commercial polymer.
2. Description of specific volume behavior outside the temperature range in which crystallization takes place, that is, fitting of isothermal compression data as given by the C-Mold database at high and low temperatures (at low temperature crystallinity

**Table III** Results of Specific Volume Measurements at Different Temperatures

Sample	Cooling Rate at 343 K (K/s)	$T$ (K)	Measurement	Specific Volume ( $\text{m}^3/\text{kg}$ )	$x$ (%) (iPP Phase) <sup>a</sup>
58	10	318	First	$1.119 \times 10^{-3}$	71
				$1.109 \times 10^{-3}$	70
				$1.098 \times 10^{-3}$	71
		298	Second	$1.117 \times 10^{-3}$	73
				$1.109 \times 10^{-3}$	71
				$1.100 \times 10^{-3}$	69
DSC0.02	0.02	318	First	$1.118 \times 10^{-3}$	72
				$1.110 \times 10^{-3}$	70
				$1.100 \times 10^{-3}$	70
		298	Second	$1.117 \times 10^{-3}$	72
				$1.110 \times 10^{-3}$	70
				$1.100 \times 10^{-3}$	69

<sup>a</sup> Crystallinity degree was calculated by eqs. (2) and (4).

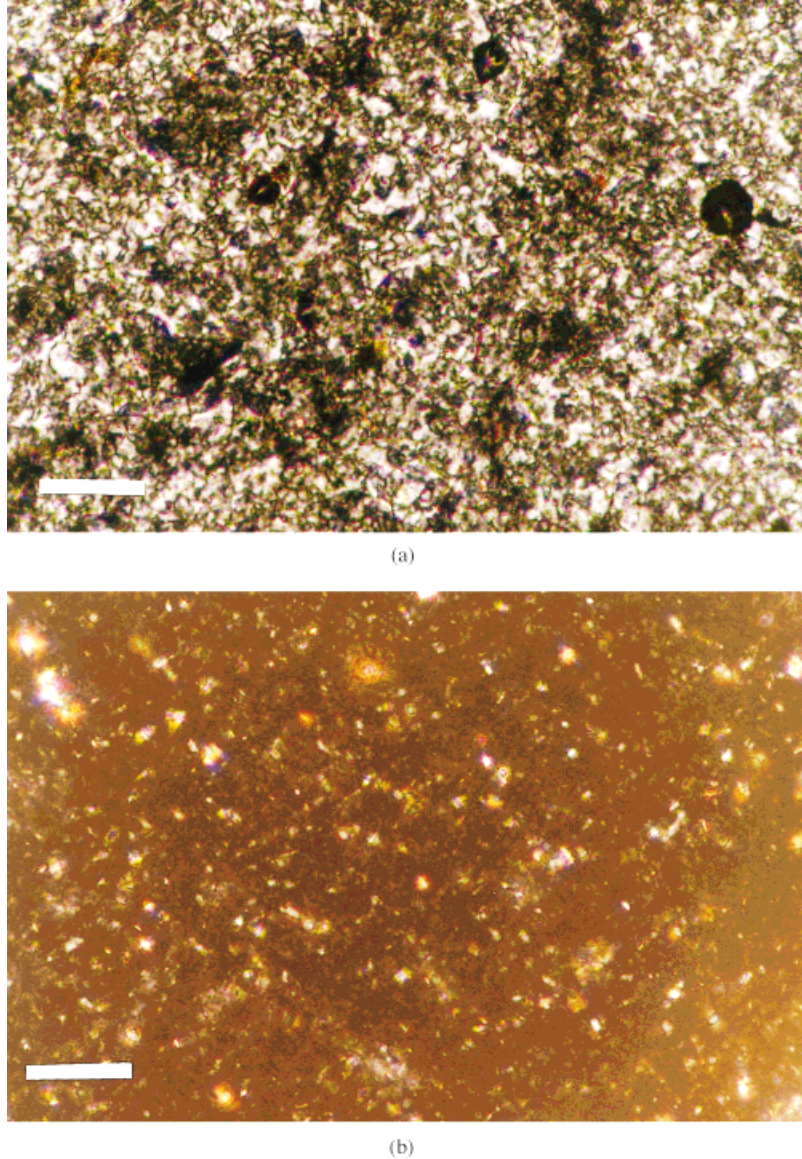


**Figure 6** Micrographs in transmitted polarized light of samples of BA 238 G3 solidified at different cooling rates. (a) Sample 1, cooling rate 0.1 K/s; (b) sample 47, cooling rate 294 K/s. Sample numbers refer to Table II. White bars are 50  $\mu$  long.

- being drawn from the calorimetric cooling ramps).
3. Description of the crystallization kinetics of the iPP phase and of specific volume behavior of the material also in the solidification temperature range on the basis of both density of quenched samples and some features of calorimetric thermograms.

#### Contribution of Phases to Specific Volume

The phases present in BA 238 G3 are iPP, EPR rubber, and talc (72.5, 26, and 1.5 wt %, respec-

tively). Assuming that phases volumes are additive in all conditions of pressure and temperature, the specific volume of the resin can be written as

$$v_{\text{BA238G3}}(T, P) = z_P v_{\text{iPP}}(T, P) + z_{\text{EPR}} v_{\text{EPR}}(T, P) + z_T v_T(T, P) \quad (2)$$

where  $v_{\text{BA238G3}}$  is the specific volume of BA 238 G3,  $v_{\text{EPR}}$  is the specific volume of the copolymer (whose mass fraction is  $z_{\text{EPR}}$ ),  $v_T$  is the specific volume of the talc (whose mass fraction is  $z_T$ ), and  $z_P$  is polypropylene mass fraction ( $z_P = 1 - z_{\text{EPR}} - z_T$ ).

**Table IV** Values of Parameters Describing Specific Volume of the Four Phases Present in Montell BA 238 G3

Phase	Mass Fraction $z$ (kg/kg)	Specific Volume at $T$ $= T^\circ$ and $P = 0$ , $v^\circ$ (m <sup>3</sup> /kg)	$T^\circ$ (K)	Thermal Expansion Coefficient $\alpha$ (1/K)	Compressibility Factor $\beta$ (1/Pa)
Talc <sup>a</sup>	1.5%	$0.370 \times 10^{-3}$	298	0	0
EPR <sup>b</sup>	26%	$1.16 \times 10^{-3}$	298	$7.70 \times 10^{-4}$	$3.8 \times 10^{-10}$
iPP Crystal <sup>c</sup>	72.5% $x^d$	$1.068 \times 10^{-3}$	298	$2.00 \times 10^{-4}$	$1.0 \times 10^{-11}$
iPP Amorphous <sup>c</sup>	72.5% (1 - $x$ )	$1.196 \times 10^{-3}$	298	$6.55 \times 10^{-4}$	$9.8 \times 10^{-10}$

<sup>a</sup> Progelhof and Throne, 1993.<sup>b</sup> Zoller and Walsh, 1995.<sup>c</sup> This study.<sup>d</sup>  $x$  = iPP crystallinity degree.

Dependence on temperature and pressure of the EPR volume can be written as

$$v_{\text{EPR}}(T, P) = v_{\text{EPR}}^\circ(1 + \alpha_{\text{EPR}}(T - T^\circ) - \beta_{\text{EPR}}P) \quad (3)$$

The parameters  $\alpha_{\text{EPR}}$  and  $\beta_{\text{EPR}}$  of an EPR of the appropriate composition (containing 50% of each component) are reported in Zoller and Walsh<sup>8</sup> and are listed in Table IV.

Dependence on temperature and pressure of talc volume is small if compared to those of other phases and thus will be neglected. The value reported in Progelhof and Throne<sup>5</sup> was then taken for  $v_T$  and is also listed in Table IV.

For the iPP phase, the analysis is carried out under the simplification that only one crystal phase forms. This is sufficient for determining the volume dependence on thermomechanical history. With such a simplification the volume of the iPP phase can be written as

$$v_{\text{iPP}}(T, P) = v_A(T, P)(1 - x) + xv_C(T, P) \quad (4)$$

where  $x$  is the volume fraction of a single equivalent crystalline phase (representing both  $\alpha$  and mesomorphic phases) within the iPP and

$$v_A(T, P) = v_A^\circ(1 + \alpha_A(T - T^\circ) - \beta_AP) \quad (5)$$

$$v_C(T, P) = v_C^\circ(1 + \alpha_C(T - T^\circ) - \beta_CP) \quad (6)$$

are specific volumes of amorphous and crystal phase, respectively.

The values of parameters of eqs. (5) and (6) were found in the course of this work by a best fit of calorimetric and density results (including the

C-Mold database); schematically, the following steps were taken:

1. Knowing the specific volume of EPR and talc phases, the specific volume of iPP phase as a function of pressure and temperature was obtained from eq. (2).
2.  $v_A^\circ$ ,  $\alpha_A$ , and  $\beta_A$  were identified by a description of volume data at high temperatures (C-Mold database): for temperatures above the transition zone (i.e.,  $T > 430$  K) volumetric curves of iPP found from eq. (4) with  $x = 0$  [i.e., from eq. (5)] should be able to describe experimental data of iPP melt [from eq. (2)], as given by the C-Mold database at all pressures.
3.  $v_C^\circ$ ,  $\alpha_C$ , and  $\beta_C$  were identified by a description of volume data at low temperatures (i.e., below 330 K) in the C-Mold database and of dilatometric measurements in density-gradient columns of the samples solidified in the DSC apparatus (of which crystallinity degree had been measured from calorimetry to be about 58%). For this purpose, it was assumed that crystallinity degree of the solid does not change (with temperature and pressure) during all tests performed at temperatures below 330 K.

Values of reference specific volume, thermal expansion coefficient, and compressibility of the iPP phase obtained as described above are also reported in Table IV.

The specific volume of the iPP phase, obtained by applying eq. (2) to the C-Mold database, is shown in Figure 7 with the high and low temperature description identified above, that is, adopt-



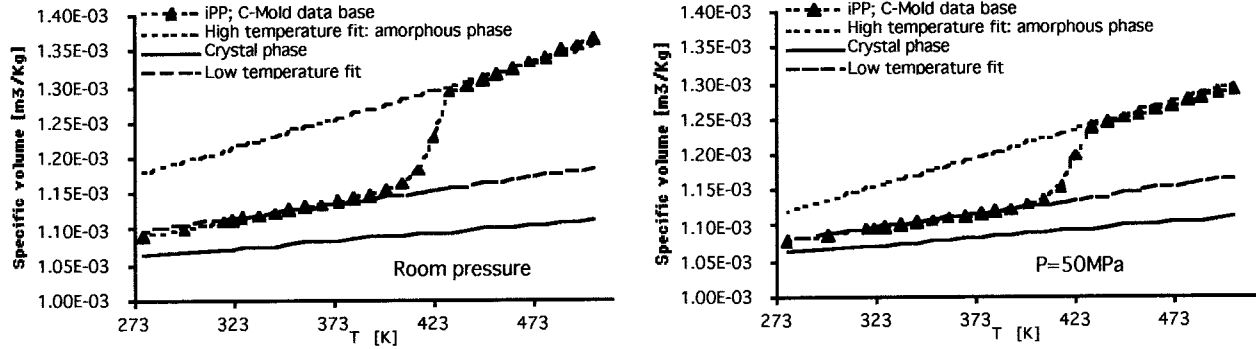


**Figure 7** Specific volume of the iPP phase as obtained applying eq. (2) to the data of the C-Mold database. High and low temperature descriptions are also shown.

ing the parameters reported in Table IV. The description is satisfactory in the high and low temperature limit. Specific volume description in the transition-temperature range is related to crystallization within the iPP phase and its kinetics. This is considered in the next section together with calorimetric results and specific volumes of quenched samples as functions of quenching cooling rates.

### Crystallization Kinetics

As mentioned earlier, at least two crystalline phases form during solidification of iPP. However, the main goal of this work is to describe PVT behavior and, for this purpose, the presence of only one equivalent crystalline phase can be considered. Crystallization kinetics within the iPP phase is considered here mainly with reference to calorimetric results and specific volumes of quenched samples as functions of quenching cooling rates. PVT description in the crystallization temperature range of the C-Mold database is considered at the end as a check of the model identified. The crystallization kinetics model adopted here is the nonisothermal formulation proposed by Nakamura et al.<sup>9</sup> of the Avrami–Evans model, which can be written

$$x = x_e \left[ 1 - \exp \left( - \ln 2 \left( \int_0^t K(T) dt \right)^n \right) \right] \quad (7)$$

where  $x_e$  is the equilibrium crystallinity value (here taken constant with temperature);  $n$  is the so-called Avrami index; and  $K(T)$  is the kinetic constant, which is a bell-shaped curve having a

maximum between melting temperature  $T_m$  and glass-transition temperature  $T_g$ . The equation

$$K(T) = K_0 \exp \left( \frac{-4 \ln 2 (T - T_{\max})^2}{D^2} \right) \quad (8)$$

which is symmetric with respect to the temperature of the maximum  $T_{\max}$ , is often adopted for  $K(T)$ . Obviously, eq. (8) holds below the crystallization temperature  $T_m$ , which is 430 K, however, as mentioned above.

The evolution of crystallinity for any of the experimental tests can be evaluated by coupling eqs. (7) and (8) with the proper thermal history. In particular, considered here for comparison with the kinetic model:

- (1) the curve of crystallization half-time during calorimetric isothermal tests as a function of temperature

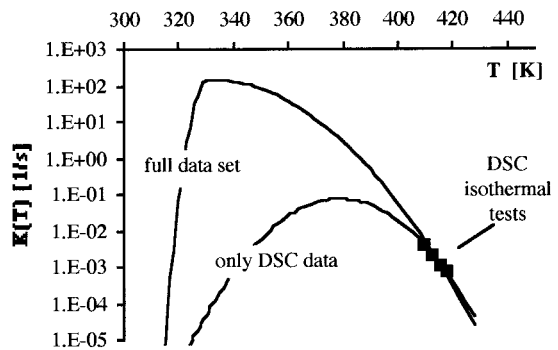


**Figure 8** Kinetic constant as expressed by eq. (8) (“Only DSC Data”) and eq. (9) (“Full Data Set”) with parameters listed in Table V. Experimental data refer to the reciprocal of crystallization half-time, drawn from curves depicted in Figure 2.

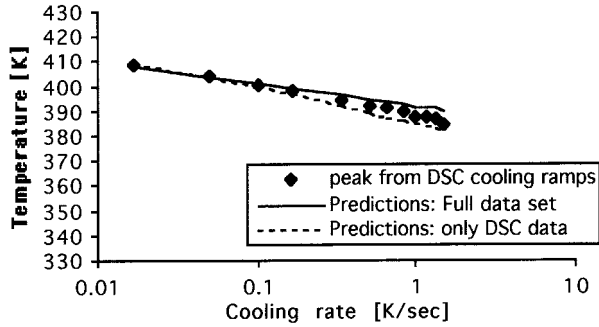


**Figure 9** Description of the peak of calorimetric curves during DSC ramps at different cooling rates, performed by means of parameters listed in Table V.

- (2) the temperature of the peak during calorimetric cooling ramps.
- (3) the final crystallinity of quenched samples

If one optimizes the five parameters ( $x_e$ ,  $n$ ,  $K_0$ ,  $T_{\max}$ ,  $D$ ) of the crystallization model with the objective of describing the above-mentioned data all together, the result is quite poor; conversely the expression for  $K(T)$  given in eq. (8) allows a good description of either final crystallinity of quenched samples or calorimetric data. The comparison between model predictions, attained adopting the values of constants identified by calorimetric data (both temperature of the peak as a function of cooling rate in the calorimeter and crystallization half-time during calorimetric isothermal tests), is shown in Figures 8 and 9 (labeled “Only DSC Data”); when temperature is constant,  $K(T)$  is equal to the reciprocal of crystallization half-time and these values are reported in the plot of  $K(T)$ . The values of the parameters are reported in Table V in the column headed “Only DSC Data.”

**Table V** Values of the Parameters Appearing in Eqs. (7), (8), and (9)

Parameter	Value	
	Only DSC Data	Full Data Set
$x_e$ ( )	58%	58%
$n$ ( )	1.25	0.35
$T_m$ (K)	430	430
$K_0$ (1/s)	0.074	148.4
$T_{\max}$ (K)	378.8	331
$D_h$ (K)	30	41
$D_l$ (K)	30	6.5

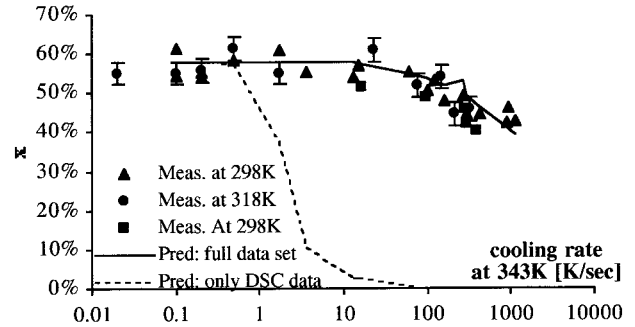


**Figure 10** Comparison of measured and predicted crystallinity degree, evaluated 10 min after solidification. Predictions performed with both sets of data presented in Table V are shown.

To achieve a good description of the complete set of data (calorimetric data and final densities of quenched samples), the function  $K(T)$  was allowed to be nonsymmetric, by adopting the expression

$$K(T) = \begin{cases} K_0 \exp\left(\frac{-4 \ln 2(T - T_{\max})^2}{D_h^2}\right) & \text{if } T_{\max} \leq T < T_m \\ K_0 \exp\left(\frac{-4 \ln 2(T - T_{\max})^2}{D_l^2}\right) & \text{if } T < T_{\max} \end{cases} \quad (9)$$

The number of parameters becomes six because there are  $D_h$  and  $D_l$ , rather than a single  $D$ . Obviously,  $K(T)$  will become symmetric if  $D_h = D_l$ . The best fit over the six parameters to the complete set of data gave rise in this case to a good result; the comparison is shown in Figures 8, 9, and 10, and the parameters are listed in Table V in the column headed “Full Data Set.”

Final specific volume of quenched samples is also compared, in Figure 11, with model predictions obtained with the set of parameters identified by fitting only DSC data (i.e., those reported in Table V as “Only DSC Data”). Although the kinetics identified, considering the complete set of data, give a reasonable description of final densities of quenched samples, the kinetics based only on DSC results completely fail to predict final crystallization degree at cooling rates higher than about 1 K/s (i.e., higher than the calorimeter’s maximum cooling rate), where predicted final crystallization degree starts to drop toward a completely amorphous sample (and a much higher final specific volume), in contrast with experimental evidence.

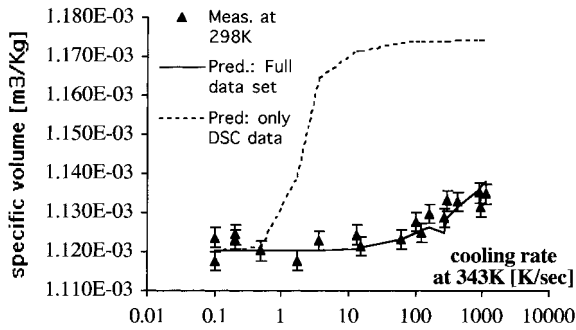


**Figure 11** Comparison of measured and predicted specific volumes after solidification. Predictions performed with both sets of data presented in Table V are shown.

Standard methods to define crystallization kinetics often rely only on calorimetric results. This is extremely dangerous and, as shown earlier, can lead to misleading results at cooling rates of a few hundred °K/s, that is, those experienced by polymers during some of the most common polymer processing operations.

Calculations of specific volume evolution can be performed by coupling thermal history with eqs. (2), (4), (7), and (9). Evolution during cooling ramps, calculated by adopting the parameters obtained considering the full set of data, is shown in Figure 12. Indeed, consistent with the data reported in Figure 1, as cooling rates increase, crystallization (and thus density changes) takes place over a wider temperature interval.

PVT behavior taken from the C-Mold database at room pressure and at 50 MPa are also reported in Figure 12: they run close to the curve calculated for a very low cooling rate (about 1 K in 1000 s). Such a slow cooling rate, however, can be consistent with the testing procedure adopted,

consisting of a series of isothermal compression volume change measurements, starting at each temperature from room pressure.

## CONCLUSIONS

An experimental procedure has been presented to describe PVT behavior of multiphase polymers in a wide range of cooling rates. The experimental procedure followed can be summarized as follows:

1. Combination of specific volume of each phase into the specific volume of the commercial polymer.
2. Description of specific volume behavior outside the temperature range where crystallization takes place, that is, fitting of standard PVT data (obtained by isothermal compression volume change measurements) at high and low temperatures.
3. Description of crystallization kinetics of the iPP phase and of specific volume behavior of the material also in the solidification temperature range, on the basis of both density of samples quenched at cooling rates of several hundreds of degrees per second and some features of calorimetric thermograms.

Following this path, a complete description of polymer PVT behavior in an extremely wide range of cooling rates can be obtained.

Polymer crystallization kinetics were described by the nonisothermal formulation proposed by Nakamura et al.<sup>9</sup> of the Avrami–Evans model. It was shown that, if one optimizes the standard five parameters of the crystallization model to the

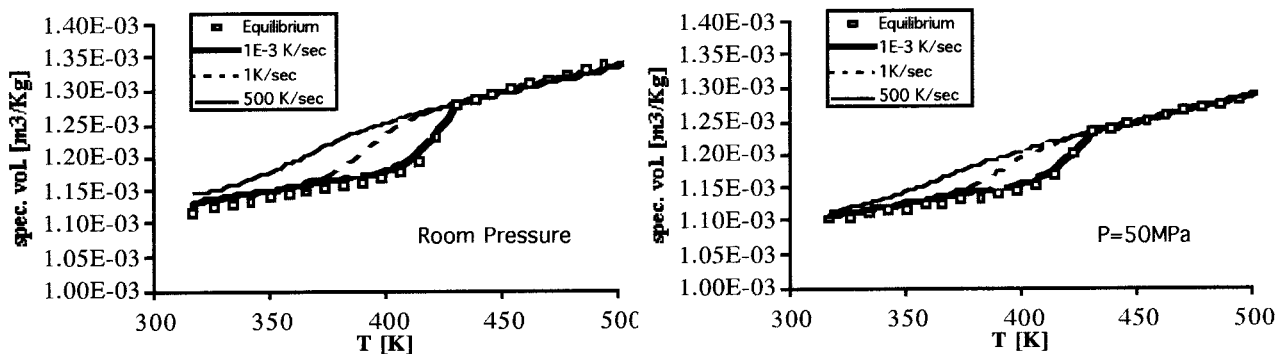


**Figure 12** Specific volume of BA 238 G3 at different cooling rates and at two pressures (0.1 and 50 MPa). Symbols refer to PVT description given in the C-Mold database.

objective of describing the above-mentioned data all together, the result is quite poor; conversely, the expression adopted for the crystallization kinetic constant  $K(T)$  gives a good description of either final crystallinity of quenched samples or calorimetric data, only. To achieve a good description of the complete set of data (calorimetric data and final densities of quenched samples), the function  $K(T)$  had to be allowed to be nonsymmetric, by introducing a sixth parameter. It was also pointed out that extrapolation of calorimetric data to cooling rates of the order of those experienced by the polymer during processing is extremely dangerous and, at the moment, a reliable model at those cooling rates can be attained only by also tuning the parameters with data relative to the cooling rates of interest.

The authors thank S. Infante for carrying out most of the experiments within her doctoral thesis in Chemical Engineering. This work was supported by CNR (Pro-

getto Finalizzato su Materiali Speciali per Tecnologie Avanzate).

## REFERENCES

1. Greener, J. *Polym Eng Sci* 1996, 26, 534.
2. Brucato, V.; Crippa, G.; Piccarolo, S.; Titomanlio, G. *Polym Eng Sci* 1991, 31, 1411.
3. Romanini, D. Personal communication.
4. C-Mold 99.1 User's Guide, Shrinkage and Warp-  
age, AC Technology, Ithaca, NY, USA; pp. 2-5.
5. Progelhof, R. C.; Throne, J. L. *Polymer Engineering Principles*; Hanser: New York, 1993.
6. Piccarolo, S.; Saiu, M.; Brucato, V.; Titomanlio, G. *J Appl Polym Sci* 1992, 46, 625.
7. Pantani, R.; Titomanlio, G. *Int J Forming Processes* 1999, 2(3-4), 211.
8. Zoller, P.; Walsh, D. J. *Standard PVT Data for Polymers*; Technomic Publishing: Lancaster, PA, 1995.
9. Nakamura, K.; Katayama, K.; Amano, K. *J Appl Polym Sci* 1973, 17, 1031.